

33 **Introduction**

34 Changes to the functions of immune cells modulate both the mammary immune microenvironment
35 and mammary epithelial cells (MEC) lineages during all stages of mammary development. For
36 example, CD4⁺ T-helper cells guide lineage commitment and differentiation of MECs, while
37 macrophages provide growth factors and assist in removal of cellular debris arising from apoptotic
38 events, during postnatal stages of mammary development (Dawson et al., 2020; Hitchcock et al.,
39 2020; Plaks et al., 2015; Rahat et al., 2016; Stewart et al., 2019; Wang et al., 2020). Accordingly,
40 changes that impact immune cell function and abundance can also influence the development
41 and progression of mammary oncogenesis (Bach et al., 2021; Ibrahim et al., 2020).

42 Immune surveillance and communication in the mammary gland are critical to post-pregnancy
43 mammary tissue homeostasis, particularly as part of mammary reconstruction during post-partum
44 involution. Alterations to immune cell composition during mammary gland involution have also
45 been suggested to influence mammary tumor progression (Lyons et al., 2011). For example, T-
46 cell activity is suppressed by the infiltration of involution-associated macrophages, an immune
47 reaction that may also induce mammary tumorigenic development (Martinson et al., 2015)(Freire-
48 de-Lima et al., 2006)(Guo et al., 2017)(Fornetti et al., 2012) (O'Brien et al., 2010).

49 Conversely, cell-autonomous processes in MECs contribute to pregnancy-induced breast cancer
50 protection, a life-long lasting effect that decreases the risk of breast cancer by ~30% in rodents
51 and humans (Medina et al., 2004)(Britt et al., 2007)(Terry et al., 2018). For example, p53 function
52 is critical for blocking mammary tumor development in murine and human MECs, with a complete
53 loss of p53 in post-pregnancy MECs promoting tumorigenic initiation (Sivaraman et al.,
54 2001)(Medina and Kittrell, 2003). Epigenetic-mediated alterations of post-pregnant MECs have
55 been shown to interfere with the transcriptional output of cMYC, which suppressed mammary
56 oncogenesis via oncogene-induced senescence (Feigman et al., 2020). Given that oncogene-
57 induced senescence signals influence the immune system, a link between normal pregnancy-
58 induced mammary development, the immune microenvironment, and oncogenesis needs to be
59 addressed to fully understand the effects of pregnancy on breast cancer development.

60 In this study, we characterize the interactions between cell-autonomous (MECs) and non-cell-
61 autonomous (immune cells) factors that occur as part of normal pregnancy-induced mammary
62 development, and that are involved in repressing cancer development in the post-involuting
63 mammary gland. Our analysis identified that pregnancy induces the expansion of a natural killer
64 T-cell (NKT) population during the late stages of involution, which preferentially populates the fully

65 involuted mammary tissue. Unlike the typical NKT cells that bear $\alpha\beta$ TCRs, mammary resident,
66 pregnancy-induced NKT cells express $\gamma\delta$ TCRs on their surface, indicating a role in specialized
67 antigen recognition. NKT cell expansion was linked with increased expression of the antigen-
68 presenting molecule, CD1d, on the surface of post-pregnancy MECs, which was associated with
69 the stable gain of active transcription markers at the Cd1d loci and increased mRNA levels.
70 Further analysis demonstrated that gain of CD1d expression on post-pregnancy MECs, and
71 expansion of $\gamma\delta$ NKT cells was observed in mammary tissues that failed to develop premalignant
72 lesions and tumors in response to oncogenic signals, such as either cMYC overexpression or loss
73 of Brca1, thus connecting pregnancy-induced molecular changes with alteration of immune
74 microenvironment and lack of mammary oncogenesis. Altogether, our findings elucidate how
75 signals brought to MECs during pregnancy-induced development regulate epigenomic changes,
76 gene expression, and immune surveillance, which together control mammary oncogenesis.

77

78 **Results**

79 **Single cell analysis identifies transcriptional programs and immune cellular heterogeneity**
80 **in mammary tissue from parous female mice**

81 The utilization of single cell strategies has elucidated the dynamics of epithelial cell lineage
82 specification and differentiation across major mammary developmental stages (Bach et al., 2017;
83 Chung et al., 2019; Li et al., 2020a; Pal et al., 2017, 2021). Previous studies have indicated that
84 post-pregnancy epithelial cells bear an altered transcriptome and epigenome, thus suggesting
85 that pregnancy stably alters the molecular state of this cell type (Blakely et al., 2006; Feigman et
86 al., 2020; Huh et al., 2015; dos Santos et al., 2015) . However, it remains unclear whether
87 pregnancy leads to disproportionate changes in the transcriptome of specific mammary cell
88 populations, which we investigated in this study.

89 In order to characterize the effects of parity on the cellular composition and heterogeneity of
90 mammary glands, we used single cell RNA-sequencing (scRNA-seq) to compare the abundance,
91 identity and gene expression of mammary gland epithelial and non-epithelial cells from nulliparous
92 (virgin, never pregnant) and parous female mice (20 days gestation, 21 days lactation, 40 days
93 post-weaning). scRNA-seq clustering defined 20 cellular clusters (TCs), which were further
94 classified into 3 main cell types; epithelial cells (Krt8+ and Krt5+), B-lymphocytes (CD20+), and
95 T-lymphocytes (CD3e+), and 2 smaller clusters, encompassing fibroblast-like cells (Rsg5+) and
96 myeloid-like cells (Itgax+), with similar cell cycle state (**Supplementary Fig. 1A-C**).

97 To characterize the cellular heterogeneity across pre- and post-pregnancy MECs, we used a re-
98 clustering approach, which selected for cells expressing the epithelial markers Epcam, Krt8,
99 Krt18, Krt14 and Krt5, and resolved 11 clusters of mammary epithelial cells (ECs) (Henry et al.,
100 2021)(**Fig. 1A**). Analysis of cellular abundance and lineage identity revealed that clusters EC7
101 (mature myoepithelial MEC), EC9 (luminal common progenitor-like MEC), EC10 and EC11 (bi-
102 potential-like MECs), were evenly represented in pre- and post-pregnancy mammary tissue, thus
103 demonstrating populations of cells that are mostly unchanged by a pregnancy cycle. We also
104 identified clusters predominantly represented within pre-pregnancy MECs (EC2, EC4, and EC8),
105 and those biased towards a post-pregnancy state (EC1, EC3, EC5, and EC6), classified as
106 luminal alveolar-like clusters (EC1, EC2 and EC6), myoepithelial progenitor-like clusters (EC3
107 and EC4), and luminal ductal-like clusters (EC5 and EC8) (**Supplementary Fig. S1D, S1E and**
108 **S1F**). Comparative gene expression analysis indicated that processes associated with immune
109 cell communication were markedly enriched in luminal and myoepithelial cell clusters biased

110 towards the post-pregnancy state (**Fig.1B, Supplementary Fig. S2A-B and Supplementary File**
111 **S1**). This observation was supported by analysis of previously published pre- and post-pregnancy
112 bulk RNA-seq data, which suggested an overall enrichment for immune communication
113 signatures in epithelial cells after a full pregnancy cycle (Feigman et al., 2020) (**Supplementary**
114 **Fig. 2C and Supplementary File S2**).

115 Changes in the immune microenvironment are known to contribute to pregnancy-induced
116 mammary development (Coussens and Pollard, 2011). A series of single cell strategies have
117 identified alterations to mammary immune composition across several stages of mammary gland
118 development and cancer development (Bach et al., 2021; Dawson et al., 2020; Saeki et al., 2021).
119 However, it still unclear whether the immune composition of fully involuted, post-pregnancy
120 mammary tissue resembles the pre-pregnancy mammary state, or whether a combination of
121 epithelial and non-epithelial signals collectively influence the normal and malignant development
122 of mammary tissue. In light of the potentially altered epithelial-to-immune cell communication
123 identified in post-pregnancy MECs suggested above, we set out to understand the effects of
124 pregnancy on the mammary resident immune compartment using scRNA-seq. Transcriptional
125 analysis of clusters representing B-lymphocytes (CD20+) did not identify major differences
126 between cells from pre- or post-pregnancy mammary glands, suggesting that B-cells may not be
127 significantly altered in fully involuted mammary tissue (**Supplementary Fig. S3A**). Re-clustering
128 of CD3e+ T-lymphocytes identified 9 distinct immune cell clusters (IC) marked by the expression
129 of immune lineage genes such as Cd4, Cd8, Klrk1, and Gzma (**Fig. 1C-D**). Interestingly,
130 classification according to cell abundance and lineage identity of pre- and post-pregnancy
131 mammary resident lymphocytes, revealed 2 cellular clusters, IC1 (CD4+ memory-like T-cells),
132 and IC2 (CD8+ T-cells), which were evenly represented across pre- and post-pregnancy
133 mammary tissue (**Supplementary Fig. S3B-C**). Differential gene expression analysis of pre- and
134 post-pregnancy T cells classified under clusters IC1 and IC2 identified minimal expression
135 changes, suggesting that the transcriptional output of CD8 T-cells (IC2), and certain populations
136 of CD4+ T-cells (IC1) were not substantially altered by parity (**Supplementary Fig. S3D-E**).

137 Analysis of clusters biased towards pre-pregnancy mammary tissue identified several populations
138 of CD4+ T-lymphocytes, with gene identifiers supporting their identity as CD4 Tregs (IC3), CD4+
139 naïve T-cells (IC7 and IC8), and CD4+ helper T-cells (IC4), suggesting pre-pregnancy mammary
140 tissues are enriched for populations of CD4+ T-cells (**Fig. 1E**). Conversely, clusters enriched with
141 post-pregnancy mammary immune cells (IC5, IC6, and IC9) were classified as NKT cells, a
142 specialized population of T-cells involved in immune recruitment and cytotoxic activity (Godfrey

143 et al., 2004) (**Fig. 1E**). Such clusters expressed master regulators of NKT cellular fate, including
144 transcription factors (TFs) Tbx21 (Tbet), and Zbtb16 (Plzf) (Townsend et al., 2004) (Savage et
145 al., 2008).

146 While Natural killer (NK) cells are known to play a role in mammary gland involution and parity-
147 associated mammary tumorigenesis (Fornetti et al., 2012; Martinson et al., 2015), the role of NKT
148 cells in this process has yet to be determined. Therefore, we set out to analyze clusters of immune
149 cells expressing the common NK/NKT marker Nkg7 in order to further define the influence of
150 pregnancy on the abundance and identity of NK and NKT cells. Deep-clustering analysis of Nkg7+
151 immune cells revealed 6 distinct cell clusters (NC1-6). Cells classified under cluster NC5, which
152 includes cells from both the pre- and post-pregnancy mammary tissue, lacked expression of
153 CD3e, and therefore was the only cluster with a NK cell identity in our dataset (**Supplementary**
154 **Fig. S4A-C**). Further gene expression analysis confirmed that post-pregnancy mammary glands
155 are enriched with a variety of NKT cells, including those expressing markers of cell activation
156 (Gzmb and Ccr5) and of a resting state (Bcl11b) (**Supplementary Fig. S4C**). In agreement, each
157 of the post-pregnancy-biased NKT cell clusters were enriched with an array of immune activation
158 signatures, suggesting an altered state for these cell populations after pregnancy
159 (**Supplementary Fig. S4D**).

160 Collectively, our scRNA-seq analysis of fully involuted mammary tissue confirmed that pregnancy
161 leads to a stable alteration of the transcriptional output of post-pregnancy MECs, including gene
162 expression signatures that suggest enhanced communication with the mammary immune
163 microenvironment. In addition, our study indicates that mammary resident NKT cells are present
164 at higher levels in post-pregnancy glands, further suggesting that pregnancy plays a role in
165 inducing changes to the mammary immune microenvironment.

166 **Pregnancy induces the expansion of a specific population of NKT cells**

167 During post-partum mammary gland involution, the immune composition of the gland expands
168 with an influx of infiltrating mast cells, macrophages, neutrophils, dendritic cells and natural killer
169 cells, which remove apoptotic epithelial cells and support the remodeling of the gland (Guo et al.,
170 2017; Kordon and Coso, 2017; O'Brien et al., 2010; Schwertfeger et al., 2001). Since our scRNA-
171 seq analyses suggested that fully involuted, post-pregnancy mammary glands are enriched for
172 populations of NKT cells, we next utilized a series of flow cytometry analyses to validate this
173 observation.

174 Analysis using antibodies against the markers NK1.1 and CD3, which defines NKT cells
175 (NK1.1+CD3+), identified a 12-fold increase in the abundance of NKT cells in post-pregnancy
176 mammary tissue, consistent with the results of our scRNA-seq data (**Fig. 2A**). Further analysis
177 indicated a 2.3-fold higher abundance of NKT cells in recently involuted mammary tissue (15 days
178 post offspring weaning), compared to mammary glands from nulliparous mice, or those exposed
179 to pregnancy hormones for 12 days (mid-pregnancy), suggesting that the expansion of NKT cells
180 is likely to initiate at the final stages of post-pregnancy mammary involution (**Supplementary Fig.**
181 **S5A**). The selective expansion of NKT cells was further supported by the analysis of markers that
182 define mammary resident neutrophils (Ly6G+), and mammary resident macrophages (CD206+),
183 which were largely unchanged between pre- and post-pregnancy mammary tissue
184 (**Supplementary Fig. S5B-C**). Immunofluorescence analysis of Cxcr6-GFP-KI mammary tissue,
185 previously described to selectively label NKT cells (Germanov et al., 2008), demonstrated several
186 GFP+ cells surrounding mammary ductal structures from pre-pregnancy mammary tissue, an
187 observation that supports the presence of NKT cells in mammary tissue (**Supplementary Fig.**
188 **S5D**). Moreover, analysis of bone marrow and spleen from nulliparous and parous mice showed
189 no difference in the abundance of NK1.1+CD3+ cells, suggesting that the pregnancy-induced
190 expansion of NKT cells is mammary-specific (**Supplementary Fig. S5E-F**).

191 To further characterize the identity of the post-pregnancy, mammary resident NKT cells, we
192 combined cell surface and intracellular staining to detect canonical NKT lineage markers,
193 including the NKT master regulator Tbet, the NKT/T-cell secreted factor IFN γ , and the NKT
194 lineage marker Nkp46 (CD335) (Yu et al., 2011). Pre- and post-pregnancy, mammary resident
195 NK1.1+CD3+ cells expressed all three markers, supporting their NKT identity. However, we
196 detected a 2-fold increase in the percentage of post-pregnancy cells expressing Tbet, IFN γ , and
197 CD335, suggesting that specific populations of NKTs are expanded in post-involuted mammary
198 tissue (**Fig. 2B**).

199 We also investigated whether pregnancy induced NKT cells represented a specialized population
200 of CD8+ T-cells, a cytotoxic cell type recently reported to reside in mammary tissues (Wu et al.,
201 2019). We found that a fraction of the NKT cells present in both pre- and post-pregnancy
202 mammary tissue expressed CD8 on their surface, accounting for 41% and 35% of the total NKT
203 cells, respectively (**Supplementary Fig. S5G**). To determine whether the triple-positive
204 (CD3+NK1.1+CD8+) cells contributed significantly to the expanded population of post-pregnancy
205 NKT cells, we analyzed mammary tissue of nulliparous and parous RAG1 KO mice, which lack
206 mature CD8+ T-cells (Mombaerts et al., 1992). We observed a 10-fold expansion of NKT cells in

207 RAG1 KO post-pregnancy mammary tissue, suggesting that CD8-expressing cells do not
208 comprise a significant fraction of pregnancy-induced NKT cells (**Supplementary Fig. S5H**).
209 These results are consistent with our scRNA-seq data, and further validate the existence of
210 specific NKT subtypes in mammary glands after a full pregnancy cycle.

211 NKT cells have multiple roles, including tissue homeostasis, host protection, microbial pathogen
212 clearance, and anti-cancer activity, mediated through their ability to recognize both foreign- and
213 self-antigens via T-cell receptors (TCRs) (Balato et al., 2009). Therefore, we next investigated
214 changes to the TCR repertoire of mammary resident, post-pregnancy NKT cells. We found that
215 17% of NKT cells expressed $\gamma\delta$ TCRs, in marked contrast to post-pregnancy NKT cells, which
216 mostly expressed $\gamma\delta$ TCR chains (44%) (**Fig. 2C, top panel**). A pregnancy cycle did not alter TCR
217 composition across all immune cells, given that mammary resident, pre- and post-pregnancy
218 CD8+ T-cells mostly express $\alpha\beta$ TCRs, suggesting that parity promotes expansion of specific
219 subtypes of NKT cells that bear a specific TCR repertoire (**Fig. 2C, bottom panel**).

220 We next investigated the molecular signatures of FACS-isolated, mammary resident, NKT cells.
221 Unbiased pathway analysis of bulk RNA-seq datasets revealed the enrichment of post-pregnancy
222 NKT cells for processes controlling overall NKT development and activation, such as Notch
223 signaling, TNF α signaling, Tgf β signaling, response to estrogen, and cMYC targets (Oh et al.,
224 2015)(Almishri et al., 2016)(Doisne et al., 2009)(Huber, 2015)(Mycko et al., 2009). Conversely,
225 pre-pregnancy NKT cells were mainly enriched for processes previously associated with reduced
226 immune activation, such as IFN α response (Bochtler et al., 2008) (**Fig. 2D, Supplementary File**
227 **S3**).

228 The activation of specific processes in post-pregnancy NKT cells was also evident from analysis
229 of their accessible chromatin landscape. ATAC-seq profiles showed similar genomic distributions
230 of accessible regions across pre- and post-pregnancy NKT cells, with a 93% overlap of their total
231 accessible chromatin regions, suggesting that parity-induced changes did not substantially alter
232 the chromatin accessibility associated with NKT lineage (**Fig. 2E and Supplementary Fig. S6A**).
233 General TF motif analysis identified chromatin accessible regions bearing classical NKT regulator
234 DNA binding motifs such as T-bet, Plzf, and Egr2, further supporting their NKT lineage identity
235 (Seiler et al., 2012) (**Supplementary Fig. S6B**). Analysis of accessible chromatin exclusively to
236 post-pregnancy NKT cells showed an enrichment for terms/genes associated with regulation of
237 the adaptive immune response, killer cell activation and antigen presentation, such as Pdk4,
238 Maged1, and Lypla1, all involved in enhanced immune-activation (Na et al., 2020)(Connaughton

239 et al., 2010)(Lee et al., 2016)(Jehmlich et al., 2013) (**Fig. 2F and Supplementary Fig. S6C**). DNA
240 motif analysis at accessible regions exclusive to post-pregnancy NKT cells identified enrichment
241 of specific TF motifs, including those recognized by MAF, a factor associated with an activated
242 NKT state, and previously predicted by our scRNA-seq data to be expressed in cell clusters with
243 an NKT identity (**Supplementary Fig. S6D**).

244 Overall, our analysis confirmed that post-pregnancy mammary tissue has an altered $\gamma\delta$ NKT cell
245 composition, which bears molecular and cellular signatures of activated and mature adaptive
246 immune cells.

247 **NKT expansion requires CD1d expression on post-pregnancy MECs**

248 Classically, NKT cells are subdivided based on their activating antigens, including the main
249 antigen-presenting molecules MHC class I, MHC class II, and the non-classical class I molecule,
250 CD1d, which can be expressed on the surface of macrophages and dendritic cells, and as well
251 on the surface of epithelial cells (Gapin et al., 2013; Rizvi et al., 2015; Thibeault et al., 2009).
252 Therefore, we next analyzed whether the expression of antigen-presenting factors on the surface
253 of mammary epithelial and non-epithelial cells could underlie NKT cell expansion after pregnancy.

254 Flow cytometry analysis detected a 5-fold increase in the CD1d levels on the surface of post-
255 pregnancy luminal and myoepithelial MECs (**Fig. 3A-B**). In contrast, no differences in the
256 expression of antigen-presenting factors MHC-I and MHC-II on the surface of pre- and post-
257 pregnancy MECs were found (**Supplementary Fig. S7A-B**). No difference in surface expression
258 of CD1d on mammary CD45+ immune cells was detected, suggesting that signals provided by
259 CD1d+ MECs could promote the post-pregnancy expansion of mammary NKT cells
260 (**Supplementary Fig. S7C**).

261 Gene expression analysis of scRNA-seq datasets and qPCR quantifications of FACS-isolated
262 epithelial cells confirmed that post-pregnancy MECs express higher levels of *Cd1d* mRNA,
263 supporting that pregnancy induced molecular alterations may represent the basis for the observed
264 increase in the percentage of CD1d+ post-pregnancy MECs (**Fig. 1D and Supplementary Fig.**
265 **S7D**). In agreement, we observed increase levels of the active transcription marker histone H3
266 lysine 27 acetylation (H3K27ac) at the *Cd1d* genomic locus in FACS-isolated post-pregnancy
267 mammary MECs, suggesting that increased mRNA levels could be associated with parity-
268 induced, epigenetic changes at the CD1d locus (**Fig. 3C**). These observations were confirmed in
269 organoid systems that mimic the transcription and epigenetic alterations brought to MECs by

270 pregnancy signals (Cicccone et al., 2020), where pregnancy hormones induced upregulation of
271 Cd1d mRNA levels and increased H3K27ac levels at the CD1d locus (**Supplementary Fig. S7E-**
272 **F**). Thus, pregnancy-associated signals may induce epigenetic alterations at the Cd1d gene
273 locus, that subsequently associate with increased *Cd1d* mRNA and CD1d protein levels in post-
274 pregnancy MECs.

275 To investigate whether CD1d expression is required for the expansion of NKT cells after parity,
276 we analyzed mammary glands from CD1d KO mice, which bear reduced levels of activated NKT
277 cells (Faunce et al., 2005; Macho-Fernandez and Brigl, 2015; Mantell et al., 2011). Mammary
278 glands from nulliparous and parous CD1d KO mice displayed similar numbers of ductal structures
279 and MEC populations as CD1d wild-type (WT) female mice, suggesting that loss of CD1d does
280 not majorly alter mammary gland tissue homeostasis (**Fig. 3D**). Further flow cytometry analysis
281 indicated no statistically significant changes in the percentage of NKT cells in mammary glands
282 of nulliparous CD1d KO mice (2.2% +/- 0.8), compared to nulliparous CD1d WT mice (3% +/- 1.6)
283 (**Fig.2A, left panel, and Fig.3E, left panel**). Conversely, we found a 7-fold decrease in the
284 percentage of NKT cells in mammary tissue from fully involuted, parous CD1d KO female mice
285 (3% +/- 1.5) compared to parous CD1d WT mammary tissue (26% +/- 4), supporting role of CD1d
286 in regulating NKT activation (**Fig.2A, right panel, and Fig.3E, right panel**). Moreover, we found
287 no difference in the abundance of NKT cells in glands from pre- and post-pregnancy CD1d KO
288 female mice, consistent with lack of Cd1d expression reducing the activation of NKT cells (**Fig.**
289 **3E**). These results were supported by the analysis of an additional mice strain that is deficient in
290 mature/activated NKT cells, due to the deletion of the histone-demethylase Kdm6 (Utx KO mouse
291 model), which failed to detect an expansion of NKT cells post-pregnancy, supporting that
292 pregnancy induces the expansion of mature/active subtypes of NKT cells (Beyaz et al., 2017)
293 (**Supplementary Fig. S7G**). Moreover, NKT cells observed in post-pregnancy CD1d KO
294 mammary tissue mainly expressed $\alpha\beta$ TCR on their surface, in contrast to the $\gamma\delta$ NKT cells
295 observed in CD1d WT post-pregnancy glands, further confirming that loss of CD1d expression
296 affects the expansion and activation of specific populations of NKT cells in post-pregnancy
297 mammary tissue (**Fig. 3F**).

298 Collectively, our studies identify pregnancy-induced epigenetic changes that may control the
299 expression of *Cd1d* mRNA in MECs, and elucidate a role for CD1d in mediating communication
300 between the MECs and the immune cell population of $\gamma\delta$ TCR-expressing NKT cells, unique to
301 post-pregnancy mammary glands.

302 **Lack of mammary oncogenesis is marked by NKT expansion and CD1d+ MECs in CAGMYC**
303 **and Brca1 KO parous female mice.**

304 Parity resulted in the expansion of a specific population of $\gamma\delta$ NKT cells in the mammary gland in
305 response to the up-regulation of CD1d on the surfaces of MECs, pointing to a mechanistic
306 connection between pregnancy-associated MECs and immune cell biology. A pregnancy has also
307 been demonstrated to induce molecular modifications to MECs associated with an oncogene-
308 induced senescence response to cMYC overexpression, and thus suppression of MEC malignant
309 transformation (Feigman et al., 2020). Therefore, we next investigated whether pregnancy-
310 induced mammary cancer protection was associated with the expansion of NKT cells.

311 Flow cytometry analysis of pre- and post-pregnancy mammary tissue from cMYC overexpressing
312 female mice (DOX-treated, CAGMYC model) demonstrated a 1.5-fold increase in the abundance
313 of total CD3+ T-cells (**Supplementary Fig. S8A**). Increased levels of CD3+ T-cell expansion was
314 also observed in mammary tissue transplanted with CAGMYC post-pregnancy MECs and
315 organoid cultures derived from post-pregnancy CAGMYC MECs, both conditions previously
316 demonstrated to lack mammary oncogenic development, and therefore suggesting a link between
317 pregnancy-induced tumorigenesis inhibition and specific changes to the adaptive immune system
318 (**Supplementary Fig. S8B-C**). This selective expansion of CD3+ T cells was further supported
319 by the analysis of markers that define mammary resident neutrophils (Ly6G+), and mammary
320 resident macrophages (CD206+), which were largely unchanged in mammary tissue transplanted
321 with either pre- and post-pregnancy CAGMYC MECs (**Supplementary Fig. S8B**).

322 Further flow cytometry analysis identified a 6-fold increase in the percentage of NKT cells in
323 mammary tissue from parous CAGMYC female mice, which predominantly expressed $\gamma\delta$ TCRs
324 (**Fig. 4A, Supplementary Fig. S8D**). No changes in the abundance of CD8+ T-cells or CD4+ T-
325 cells was observed between mammary tissue from nulliparous and parous CAGMYC female
326 mice, supporting the parity-induced expansion of $\gamma\delta$ NKT cells (**Supplementary Fig. S8E-F**), and
327 suggesting that specific constituents of the mammary immune microenvironment may control
328 mammary tumorigenesis. In agreement, we also found a 5-fold higher percentage CD1d+ luminal
329 MECs in post-pregnancy mammary tissue, thus linking gain of CD1d expression and the
330 expansion of $\gamma\delta$ TCR-expressing NKT cells, which may collectively play a role in blocking
331 tumorigenesis (**Fig. 4B**).

332 cMYC overexpression is present in approximately 60% of basal-like breast cancers, with cMYC
333 gain of function commonly found in BRCA1 mutated breast cancers (Chen and Olopade, 2008;

334 Grushko et al., 2004). Interestingly, women harboring *BRCA1* mutations with a full-term
335 pregnancy before the age of 25 benefit from pregnancy-induced breast cancer protection (Medina
336 et al., 2004; Terry et al., 2018). Therefore, we developed an inducible mouse model of *Brca1* loss
337 of function, for the purpose of investigating how pregnancy-induced changes influences *Brca1*
338 null mammary tumor development. In this model, tamoxifen (TAM) induces homozygous loss of
339 *Brca1* function in cells that express the cytokeratin 5 gene (*KRT5*⁺ cells), which include MECs
340 (dos Santos et al., 2013), cells from gastrointestinal tract (Sulahian et al., 2015), reproductive
341 organs (Ricciardelli et al., 2017), and additional epithelial tissue (Castillo-Martin et al., 2010;
342 Majumdar et al., 2012), in *p53* heterozygous background (*Krt5*^{CRE-ERT2}*Brca1*^{fl/fl}*p53*^{-/+}, hereafter
343 referred as *Brca1* KO mouse).

344 Nulliparous *Brca1* KO mice exhibited signs of mammary hyperplasia approximately 12 weeks post
345 TAM treatment, which gradually progressed into mammary tumors at around 20 weeks after
346 *Brca1* deletion (**Supplementary Fig.S9A-B**). *Brca1* KO mammary tumors display cellular and
347 molecular features similar to those previously described in human breast tissue from *BRCA1*
348 mutant carriers and animal models of *Brca1* loss of function, including high EGFR and *KRT17*
349 protein levels and altered copy number variation marked by gains and losses of genomic regions
350 (**Annunziato et al. Nat Comm. 2019**) (**Supplementary Fig.S9C-D**).

351 To investigate the effects of pregnancy on the mammary immune microenvironment and
352 mammary oncogenesis, age matched, TAM-treated, *Brca1* KO nulliparous female mice, and
353 parous *Brca1* KO female mice (1 pregnancy, 21-days of gestation, 21-days of lactation/nursing,
354 and 40-days post offspring weaning) were monitored for tumor development (**Supplementary**
355 **Fig.S10A**). Our study demonstrated that 100% of all nulliparous *Brca1* KO female mice (5 out of
356 5 mice) developed mammary tumors, compared to only 20% of the parous *Brca1* KO female mice
357 that developed mammary tumors (1 out of 5), thus indicating that a full pregnancy cycle decreases
358 the frequency of *Brca1* KO mammary tumors by 80% (**Fig. 4C-D**).

359 Histo-pathological analysis suggested that pre-pregnancy mammary tumors were quite diverse
360 as previously reported for tumors from *Brca1* KO mice (Brodie et al., 2001). These included poorly
361 differentiated tumors, such as micro-lobular carcinomas with squamous trans-differentiation (**Fig.**
362 **4D – top rows, far left panel**), medullary like carcinomas (**Fig. 4D – top rows, right panel**), and
363 solid carcinomas resembling high-grade invasive ductal carcinoma (IDC) in humans (**Fig. 4D –**
364 **top rows, left and far right panels**). Accordingly, the only tumor-bearing parous *BRCA1* KO
365 female mouse developed a poorly differentiated carcinoma with extensive squamous trans-

366 differentiation and with extensive necrosis, also previously reported for tumors from Brca1 KO
367 mice (**Fig. 4D – bottom rows, far right panels**). Additional histo-pathological analysis confirmed
368 that mammary tissues from the remaining parous Brca1 KO female mice (4 out of 5) were largely
369 normal (**Fig. 4D – bottom rows, far left, left and right panels and Supplementary Fig. S10B**).
370 Immunofluorescence analysis confirmed that both pre-pregnancy mammary tumors and post-
371 pregnancy normal mammary tissue were indeed deficient for KRT5+BRCA1+ epithelial cells,
372 indicating that the lack of mammary tumors in parous female mice was not due to inefficient Brca1
373 deletion (**Supplementary Fig. S11A**).

374 Flow cytometry analysis of Brca1 KO MECs demonstrated a progressive loss of myoepithelial
375 cells in tumor tissue from nulliparous (2.5-fold) and parous (2-fold) Brca1 KO female mice, defined
376 by an increase in the percentage of CD24^{high}CD29^{low} luminal-like MECs, (**Supplementary Fig.**
377 **S11B**). These results suggest that tumor progression in this model is accompanied by changes
378 to the population of CD24^{high} MECs, which has been associated with poor clinical outcomes in
379 patients with triple negative breast cancer (Chan et al., 2019). Further cellular analysis indicated
380 a 2.7-fold increase in the percentage of CD24^{high}/luminal cells CD1d+ cells in healthy, post-
381 pregnancy Brca1 KO mammary tissue compared to tissue from tumor-bearing nulliparous Brca1
382 KO mice and parous Brca1 KO mice, supporting that parity induces the expression of CD1d at
383 the surface of MECs (**Fig.4E**).

384 Given the increased levels of CD1d expression at the surface of post-pregnancy Brca1 KO MECs,
385 we next investigated the presence of NKT cells in mammary tissue from nulliparous and parous
386 Brca1 KO female mice. Flow cytometry analysis demonstrated a 3.8-fold increase in the
387 percentage of NKT cells in healthy, post-pregnancy Brca1 KO mammary tissue compared to non-
388 affected normal mammary tissue from tumor-bearing, nulliparous Brca1 KO mice and parous
389 Brca1 KO mice (**Fig.4F and Supplementary Fig. S11C**). Additional flow cytometry analysis
390 demonstrated that approximately 70% of total NKT cells from healthy, post-pregnancy Brca1 KO
391 mammary tissue expressed $\gamma\delta$ TCR, in marked contrast to NKT cells from healthy (2.7%) and
392 tumor mammary tissue (8.6%) from nulliparous Brca1 KO mice (**Fig.4G**).

393 Collectively, our findings show that pregnancy-induced gain of CD1d expression at the surface of
394 MECs and expansion of NKT cells associates with lack of mammary oncogenesis in response to
395 cMYC overexpression or loss of Brca1 function, thus supporting to the link between pregnancy-
396 induced molecular changes, mammary tissue immune alteration, and inhibition of mammary
397 tumorigenesis in clinically relevant mouse models.

398 **Functionally active NKT cells are required to block malignant progression of post-**
399 **pregnancy MECs**

400 Given that we demonstrated that pregnancy-induced changes block mammary oncogenesis in
401 two distinct models (**Fig.4**), and that cMYC gain of function is commonly found in BRCA1 mutated
402 breast cancers, we utilized the cMYC overexpression model to further characterize the effects of
403 the immune microenvironment on the malignant progression of post-pregnancy MECs. Analysis
404 of fat-pad transplantations into severely immune deficient NOD/SCID female mice, which lack T-
405 cells, B-cells, NK and NKT cells, indicated that 100% of mammary tissue injected with pre-
406 pregnancy (n=5) or post-pregnancy (n=5) CAGMYC MECs developed adeno-squamous-like
407 carcinomas with acellular lamellar keratin, high levels of cell proliferation (Ki67 staining), and
408 increased collagen deposition (Trichrome blue staining) (**Supplementary Fig. S12A-C**).
409 Therefore, NKT cells, or associated adaptive immune cells, are required for the parity associated
410 protection from oncogenesis in the CAGMYC model.

411 Bulk RNA-seq analysis demonstrated that post-pregnancy CAGMYC MECs transplanted into the
412 fat-pad of NOD/SCID female mice were less effective at activating the expression of canonical
413 cMYC targets and estrogen response genes, compared to transplanted pre-pregnancy CAGMYC
414 MECs, in agreement with the previously reported transcriptional state of post-pregnancy
415 CAGMYC MECs (Feigman et al., 2020) (**Supplementary Fig. S12D**). We also found that
416 organoid cultures derived from post-pregnancy CAGMYC MECs transplanted into NOD/SCID
417 female mice retained a senescent-like state, characterized by reduced p300 protein levels and
418 moderately increased p53 protein levels, in agreement with the previously reported senescence
419 state of post-pregnancy CAGMYC MECs (Feigman et al., 2020) (**Supplementary Fig. S12E**).
420 Together, these findings indicate that oncogenic progression of post-pregnancy CAGMYC MECs
421 is associated with the immune deficient mammary microenvironment of NOD/SCID mice.

422 While our investigation of post-pregnancy CAGMYC MECs that were transplanted into the
423 mammary tissue of immunosuppressed animals alluded to the importance of a robust immune
424 system in blocking mammary tumor development, it did not uncouple whether functionally active
425 NKT cells, or CD1d expression at the surface of MECs, act to block oncogenesis in post-
426 pregnancy mammary tissue. Therefore, to determine whether signaling between CD1d+ MECs
427 and NKT cells is critical for the development of mammary oncogenesis after pregnancy, we
428 developed a double transgenic mouse model, by crossing the DOX-inducible CAGMYC mice into
429 a CD1d KO background, hereafter referred as CAGMYC CD1d KO.

430 Tissue histology analysis indicated that mammary tissue from DOX-treated, nulliparous and
431 parous CAGMYC CD1d KO female mice showed signs of tissue hyperplasia with atypia and
432 abnormal ductal structures, demonstrating that loss of Cd1d expression is accompanied by
433 mammary oncogenesis in a parity-independent fashion (**Fig. 5A, left and far right panels and**
434 **Supplementary Fig. S13A**). Conversely, analysis of DOX-treated, CAGMYC CD1d WT mice
435 showed that mammary tissue from parous female mice lacked malignant lesions in response to
436 cMYC overexpression (**Fig. 5A, right panels and Supplementary Fig. S13A**). Flow cytometry
437 analysis showed a lack of NKT cells in mammary tissue from both nulliparous and parous
438 CAGMYC CD1d KO female mice, in marked contrast to the observed expansion of $\gamma\delta$ NKT cells
439 in healthy post-pregnancy CAGMYC CD1d WT mammary glands that lacked tissue hyperplasia
440 development, suggesting that CD1d expression may control pregnancy-induced
441 expansion/activation of NKTs, and thus block of mammary tumorigenesis. (**Supplementary Fig.**
442 **S13B and Fig.4A**). To further determine whether loss of CD1d expression underlies the malignant
443 transformation of post-pregnancy CAGMYC MECs, we performed mammary transplantation
444 assays of CAGMYC CD1d KO MECs into the fat-pad of syngeneic animals (CD1d WT female
445 mice). We found that 100% of mammary tissue injected with pre-pregnancy CAGMYC CD1d KO
446 MECs and 70% of mammary glands injected with post-pregnancy CAGMYC CD1d KO MECs
447 developed signs of malignant lesions, supporting that the loss of CD1d expression impacts
448 pregnancy-induced breast cancer protection (**Fig. 5B - black font, and Supplementary Fig.**
449 **S13C-D**). This last observation was in marked contrast to the finding in glands injected with post-
450 pregnancy CAGMYC CD1d WT MECs, which as previously reported did not present signs of
451 malignant transformation (Feigman et al., 2020) (**Fig. 5B, blue font and Supplementary Fig.**
452 **S13E-F**).

453 Altogether, these results suggest that loss of CD1d, with concomitant loss of pregnancy-induced
454 expansion of NKT cells, supports the development of mammary malignant lesions, independently
455 of parity. Moreover, our study elucidates that parity blocks the malignant transformation of MECs,
456 both by inducing cell-autonomous, epigenetic alterations within the MECs, and non-autonomous,
457 communication between CD1d+ MECs cells and NKT cells in the mammary gland.

458 **Discussion**

459 In mammals, reprogramming of the immune system is initiated after birth, and continues
460 throughout the lifespan of an individual due to exposure to pathogens, hormonal fluctuations, and
461 aging. This dynamic reprogramming is part of an immune surveillance system that detects

462 abnormal cells across many tissues, helping to prevent cancer. Here, we characterized a
463 population of mammary resident NKT immune cells in post-pregnancy mammary tissue, and it's
464 role on inhibiting mammary oncogenesis

465 Our findings suggest that post-pregnancy mammary homeostasis does not rely on the presence
466 of $\gamma\delta$ NKT cells, given the largely normal histology and cellular content of mammary tissue in mice
467 deficient for this cell type. It is possible that NKT cells expand in response to the re-setting of
468 whole-body immunity post-partum, with the child-bearing event providing signals that alters
469 antigens across all maternal tissues as well as expanding specific immune cell populations.
470 $\gamma\delta$ NKT cells have been found in the pregnant uterus across many mammalian species, linking
471 NKT specialization and the pregnancy cycle (Mincheva-Nilsson, 2003). Our results support that
472 the expansion of NKT cells was predominantly observed in post-lactating, post-involution tissue,
473 thus suggesting that the immune reprogramming of mammary tissue takes place after giving birth.
474 In addition to the NKT cell population expansion, parity also promotes a modification of the TCR
475 repertoire in NKT cells. $\gamma\delta$ T-cells reside within the normal breast, and their presence has been
476 associated with a better prognosis during triple-negative breast cancer development (Wu et al.,
477 2019). Here we report that pregnancy-induced changes in TCR expression was specific to NKT
478 cells, given that we did not find pregnancy-induced TCR rearrangements in CD8+NK1.1- immune
479 cells, pointing to the specific engagement of NKT-lineages during pregnancy-induced mammary
480 development.

481 Several other immune subtypes have been described to be enriched in mammary tissue during
482 gestation, lactation and post-pregnancy involution stages of mammary gland development. These
483 studies identified alterations in leukocyte interaction with mammary ductal structures, as well to
484 specific transcriptional changes, suggesting that cell interaction and cellular identity of mammary
485 resident cells are affected by pregnancy-induced development (Dawson et al., 2020; Hitchcock
486 et al., 2020). Our analysis of leukocytes, specifically macrophages and neutrophils, did not show
487 alterations in cell abundance, neither in mammary tissue from healthy parous female mice, nor in
488 post-pregnant CAGMYC mammary tissue lacking malignant lesions. Moreover, we found that
489 CD1d expression on the surface of total CD45+ mammary resident immune cells were not altered
490 by parity, thus supporting a role for post-pregnancy CD1d+ MECs in regulating CD1d-dependent
491 NKT cells. However, given that leukocytes have been implicated in the activation of NKT cells
492 (Macho-Fernandez and Brigl, 2015; Rizvi et al., 2015), it is possible that molecular alterations,
493 rather than changes to cellular abundance or antigen presentation, could play a role in inducing
494 or sustaining the population of NKT cells in post-pregnancy mammary tissue.

495 Our studies also provide evidence linking pregnancy-induced immune changes with the inhibition
496 of mammary oncogenesis. Our previous research focused on how post-pregnancy MECs assume
497 a senescence-like state in response to cMYC overexpression, an oncogene-induced response
498 that activates the immune system via the expression of senescence-associated genes (Braig and
499 Schmitt, 2006). Here, we found that CD1d expression at the surface of post-pregnancy MECs,
500 and the presence of $\gamma\delta$ NKT cells were linked with the inhibition of mammary oncogenesis in two
501 independent models of breast cancer, illustrating how epithelial and immune cells communicate
502 to support pregnancy-induced mammary cancer prevention. Given that NKT cells were previously
503 shown to interact with senescent cells, it is possible that pregnancy-induced activation of CD1d
504 expression and NKT cell expansion represent additional responses to oncogene-induced cellular
505 senescence (Kale et al., 2020).

506 Women completing a full-term pregnancy before the age of 25 have a substantially reduced breast
507 cancer risk, by approximately one-third (Medina et al., 2004). This benefit applies to the risk of all
508 breast cancer subtypes, including those from women harboring *BRCA1* mutations (Terry et al.,
509 2018). Thus, our findings supporting a role for pregnancy in inhibiting the development of Brca1
510 KO mammary tumors lends a clinical relevance to our studies. Interestingly, mammary tumor from
511 parous Brca1 KO female mouse was associated with low abundance of $\gamma\delta$ NKT cells and CD1d+
512 MECs, suggesting that loss of the pregnancy-induced epithelial to immune microenvironment
513 communication may support mammary tumorigenesis. In agreement, the genetically engineered
514 loss of CD1d expression, with a consequent deficiency in activated NKTs, supported the
515 malignant progression of cMYC overexpressing MECs, thus further illustrating a link between
516 epithelial and immune cells in supporting pregnancy-induced mammary cancer prevention.

517 Our findings are based on studies performed in mice that became pregnant at a young age (~8
518 weeks old), which reinforced pregnancy-induced changes to epithelial cells, and their effect on
519 immune recruitment and oncogenesis inhibition. However, it remains unclear why such strong,
520 pregnancy-induced changes do not fully prevent the development of breast cancer (Nichols et al.,
521 2019). It has been suggested that specific mammary epithelial clones with oncogenic properties
522 reside within the mammary tissue after pregnancy, and may give rise to late-onset mammary
523 oncogenesis in aged mice (Li et al., 2020b). It is possible that such populations of rare MECs lose
524 some of their pregnancy-induced molecular signatures over time, thereby bypassing oncogene-
525 induced senescence and immune recognition, and ultimately developing into mammary tumors.
526 Moreover, and given that pregnancy-induced breast cancer protection becomes apparent ~5-8-
527 years after pregnancy, it is possible that additional immune reprogramming induced by genetic

528 makeup, age at pregnancy, and/or overall post-partum health, may further modify breast tissue
529 and erase pregnancy-induced changes that inhibit breast cancer development.

530 Nonetheless, the connection between pregnancy, immunity, and oncogenesis could be used to
531 develop therapies to block cancer development. For example, strategies could be developed to
532 induce NKT expansion in the absence of a true pregnancy. Indeed, a series of preclinical models
533 have been developed to optimize the delivery of CD1d stimulatory factors, such as α Galcer and
534 KRN7000, and induce expansion of NKT cells (Zhang et al., 2019). Such strategies are mostly
535 side-effect free, and could be used in cases of high cancer risk, including in the event of genetic
536 alterations that affect Brca1 function and/or family history of breast cancer. Additionally, the
537 characterization of specific, pregnancy-induced TCR rearrangements could be leveraged in CAR-
538 NKT immunotherapy, for example, which could also efficiently target disease that has already
539 developed. Collectively, such strategies could also improve breast health, nursing experience,
540 and decrease cancer risk in women that experience their first pregnancy after 35 years of age,
541 when they are at greater risk of requiring medical intervention to improve milk production and
542 breastfeeding assistance and to develop breast cancer.

543

544 **Acknowledgements.** This work was performed with assistance from CSHL Animal Facility, the
545 CSHL Tissue Histology Shared Resources, the CSHL NextGen Sequencing Shared Resources,
546 the CSHL Single Cell Shared Resources, the CSHL Flow Cytometry Shared Resources, and the
547 CSHL Microscopy Shared Resources, which are supported by the CSHL Cancer Center Support
548 Grant 5P30CA045508. This work was financially supported by the CSHL and Northwell Health
549 affiliation, the CSHL and Simons Foundation Award, the Rita Allen Scholar Award, the Pershing
550 Square Sohn Prize for Cancer Research, the Breast Cancer Research Foundation, the NIH/NCI
551 grant R01CA248158-01, and the NIH/NIA grant R01 AG069727-01 (C.O.D.S.). Whole genome
552 sequencing (CNV analysis) was performed with financial support provided to Dr. Michael Wigler
553 by The Breast Cancer Research Foundation (BCRF-19-174) and Simons Foundation, Life
554 Sciences Founder Directed Giving-Research (519054). We would like to thank Dr. Douglas
555 Fearon for critical feedback, and Mrs. Shih-Ting Yang for the mouse illustrations.

556 **Author contributions.** C.O.D.S. designed and supervised the research; C.O.D.S., A.V.H.S.,
557 M.A.M., M.J.F., and S.L.C. wrote the manuscript. A.V.H.S., M.A.M., M.J.F., C.C., S.L.C., M.F.C.,
558 M.C.T, and M.V. performed experiments and analyzed results. M.A.M, and M.C.T. performed
559 bioinformatics analyses. S.L., and J.K., performed and analyzed whole genome sequencing (CNV
560 analysis). S.B. provided reagents and critical feedback. J.E.W. performed histopathological

561 analysis.

562 **Declaration of Interests.** The authors have no competing interests to disclose.

563 **Resource availability.**

564 **Materials Availability.** All unique/stable reagents generated in this study are available from the
565 Lead Contact with a completed Materials Transfer Agreement.

566

567 **Data and Code Availability.** scRNA-seq, RNA-seq, ATAC-seq datasets were deposited into
568 BioProject database under number PRJNA708263, and will be made available upon manuscript
569 acceptance/publication. Whole genome sequencing datasets were deposited under number
570 SUB10186897. Results shown in Figure 1 (pre-pregnancy scRNA-seq) were previously deposited
571 under number SUB8429356 (data pending release). Results shown in Supplementary Fig. S2C
572 (pre- and post-pregnancy RNA-seq), Fig.3C (pre- and post-pregnancy H3K27ac ChIP-seq) were
573 previously deposited in the BioProject database under numbers PRJNA192515
574 [<https://www.ncbi.nlm.nih.gov/bioproject/?term=PRJNA192515>] and PRJNA544746
575 [<https://www.ncbi.nlm.nih.gov/bioproject/PRJNA544746>]. Results shown on Supplementary Fig.
576 S7F (H3K27ac Cut&Run of organoid cultures) was previously deposited in the BioProject
577 database under number PRJNA656955
578 (<https://www.ncbi.nlm.nih.gov/sra/?term=PRJNA656955>).

579 **Experimental model and subjects details**

580 **Animal Studies.** All experiments were performed in agreement with approved CSHL Institutional
581 Animal Care and Use Committee (IACUC). All animals were housed at a 12 hour light/12 hour
582 dark cycle, with a controlled temperature of 72°F and 40-60% of humidity. Balb/C female mice
583 were purchased from The Jackson Laboratory and Charles River. RAG1 KO mice (B6.129S7-
584 Rag1^{tm1Mom/J}, IMSR Cat# JAX:002216, RRID:IMSR_JAX:002216) were purchased from The
585 Jackson Laboratory. VavCre UTX KO were generated as previously described (Beyaz et al.,
586 2017). CXCR6-KO-EGFP-KI mice (B6.129P2-Cxcr6^{tm1Litt/J}, IMSR Cat# JAX:005693,
587 RRID:IMSR_JAX:005693) were purchased from The Jackson Laboratory. CAGMYC transgenic
588 mouse strain was generated as previously described (Feigman et al., 2020). CD1d KO CAGMYC
589 transgenic mouse strain was generated by crossing CD1d KO (C.129S2-Cd1^{tm1Gru/J}, IMSR Cat#
590 JAX:003814, RRID:IMSR_JAX:003814) mice with CAGMYC mice. Krt5^{CRE-ERT2}Brca1^{fl/fl}p53^{het}
591 (Brca1 KO) transgenic mouse strain was generated by crossing Blg^{CRE}Brca1^{fl/fl}p53^{het} transgenic

592 mouse strain (Trp53^{tm1Brd}Brca1^{tmAash}Tg(B-cre)74Acl/J, IMSR Cat# JAX:012620,
593 RRID:IMSR_JAX:012620) with Krt5^{CRE-ERT2} transgenic mouse strain (B6N.129S6(Cg)-
594 Krt5^{tm1.1(cre/ERT2)Blh}/J, IMSR Cat# JAX:029155, RRID:IMSR_JAX:029155).

595 **Methods details.** Full description of methods is provided as Supplementary Information.

596

597

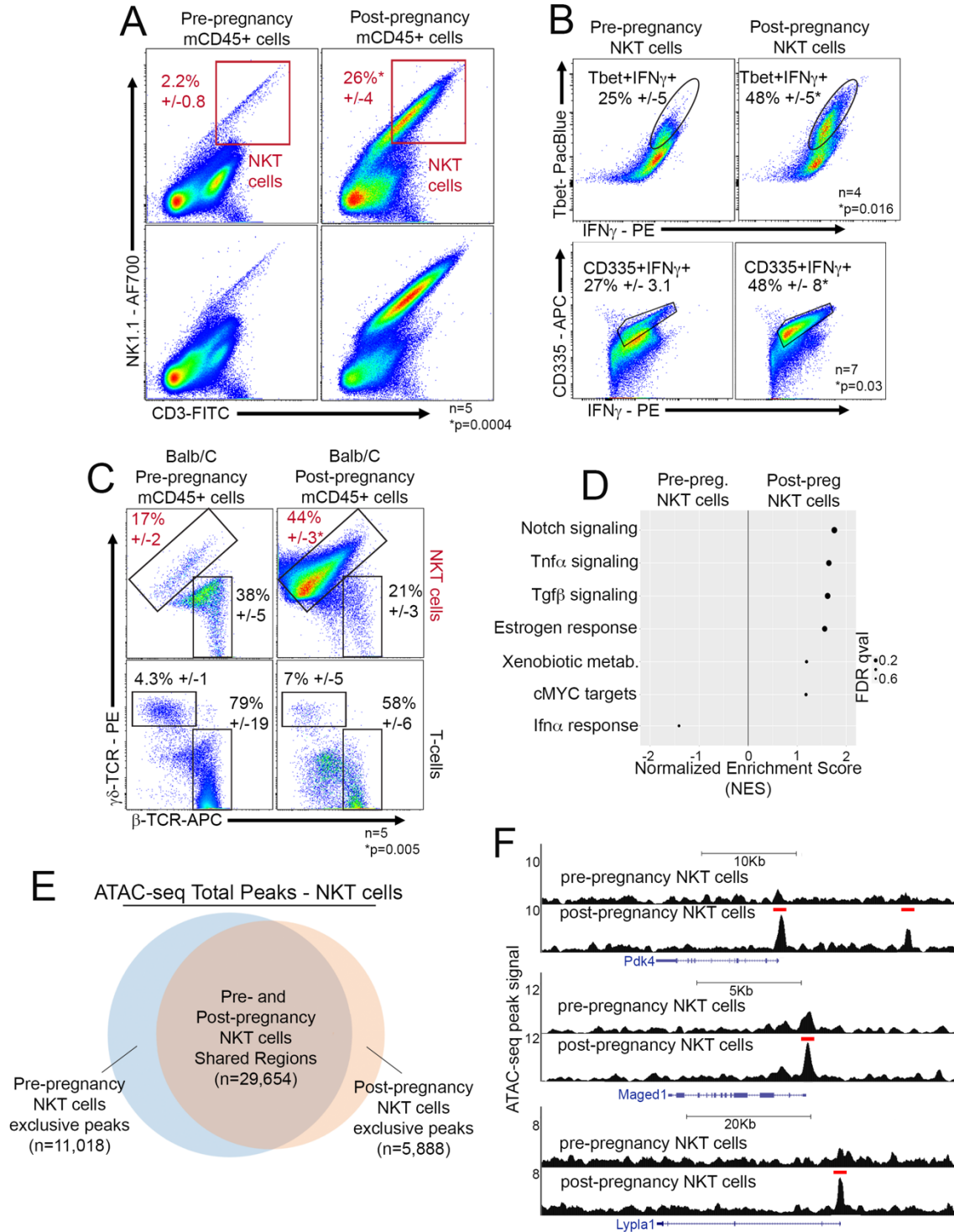
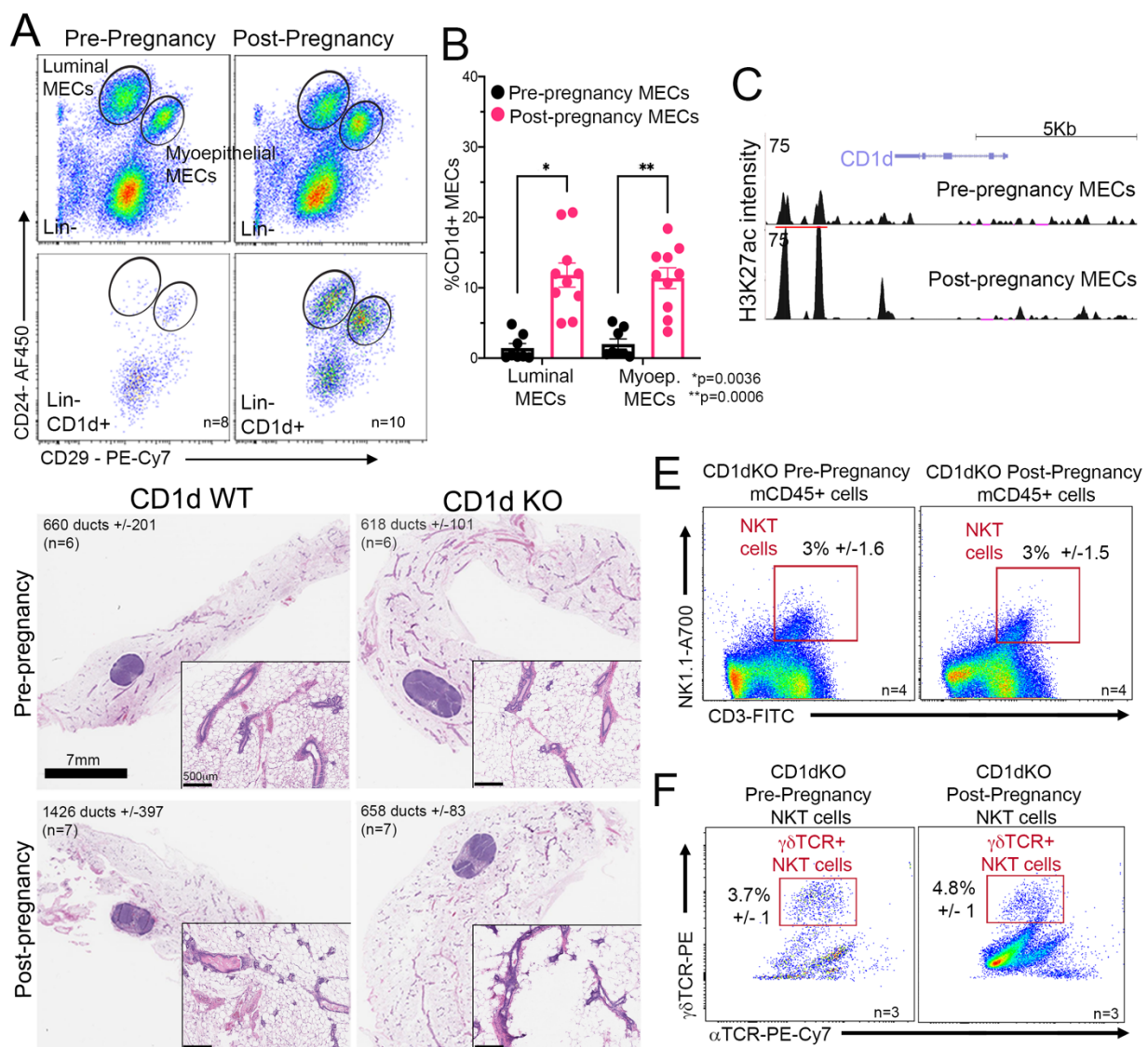


Figure 2

600

601

602



603

Figure 3

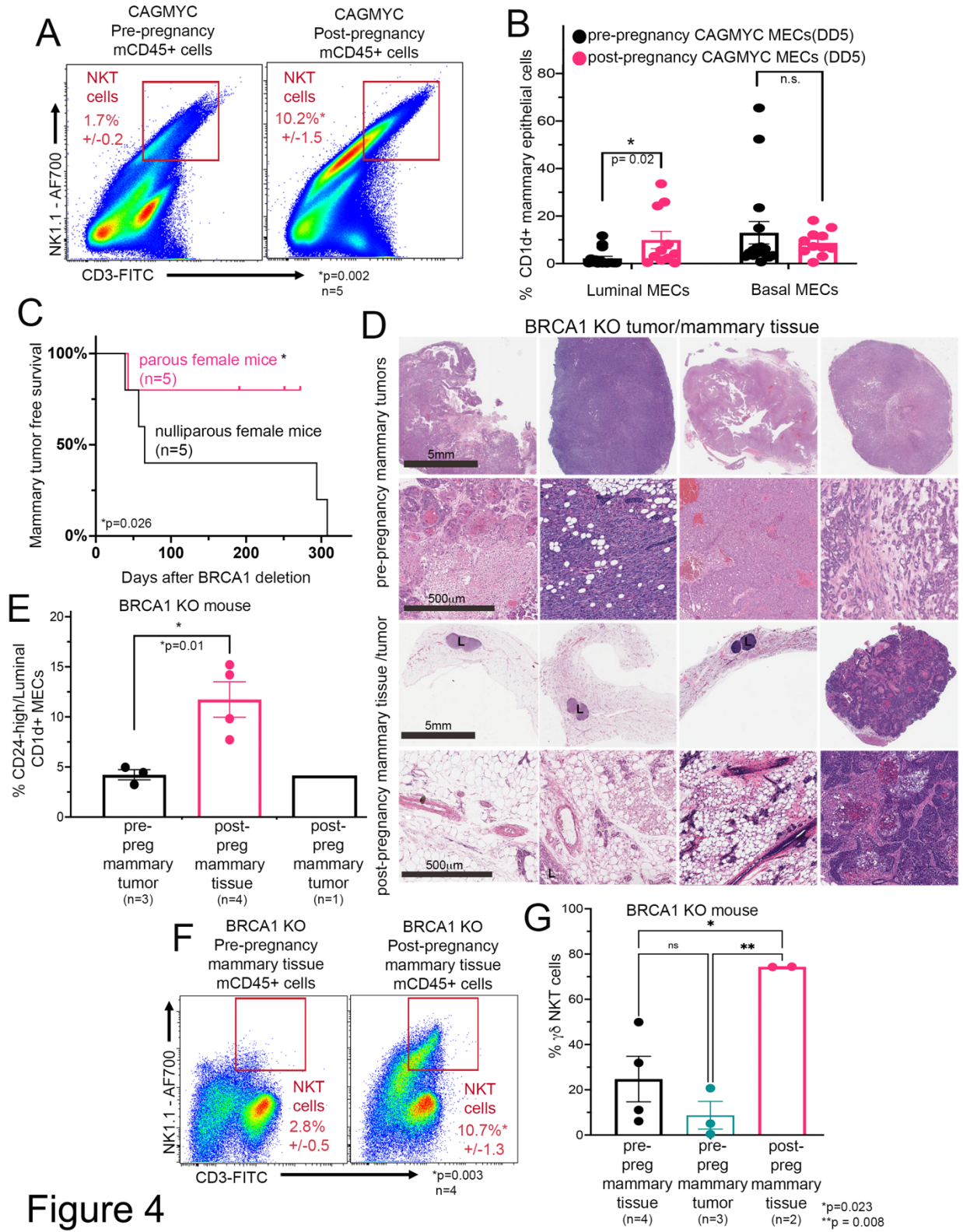
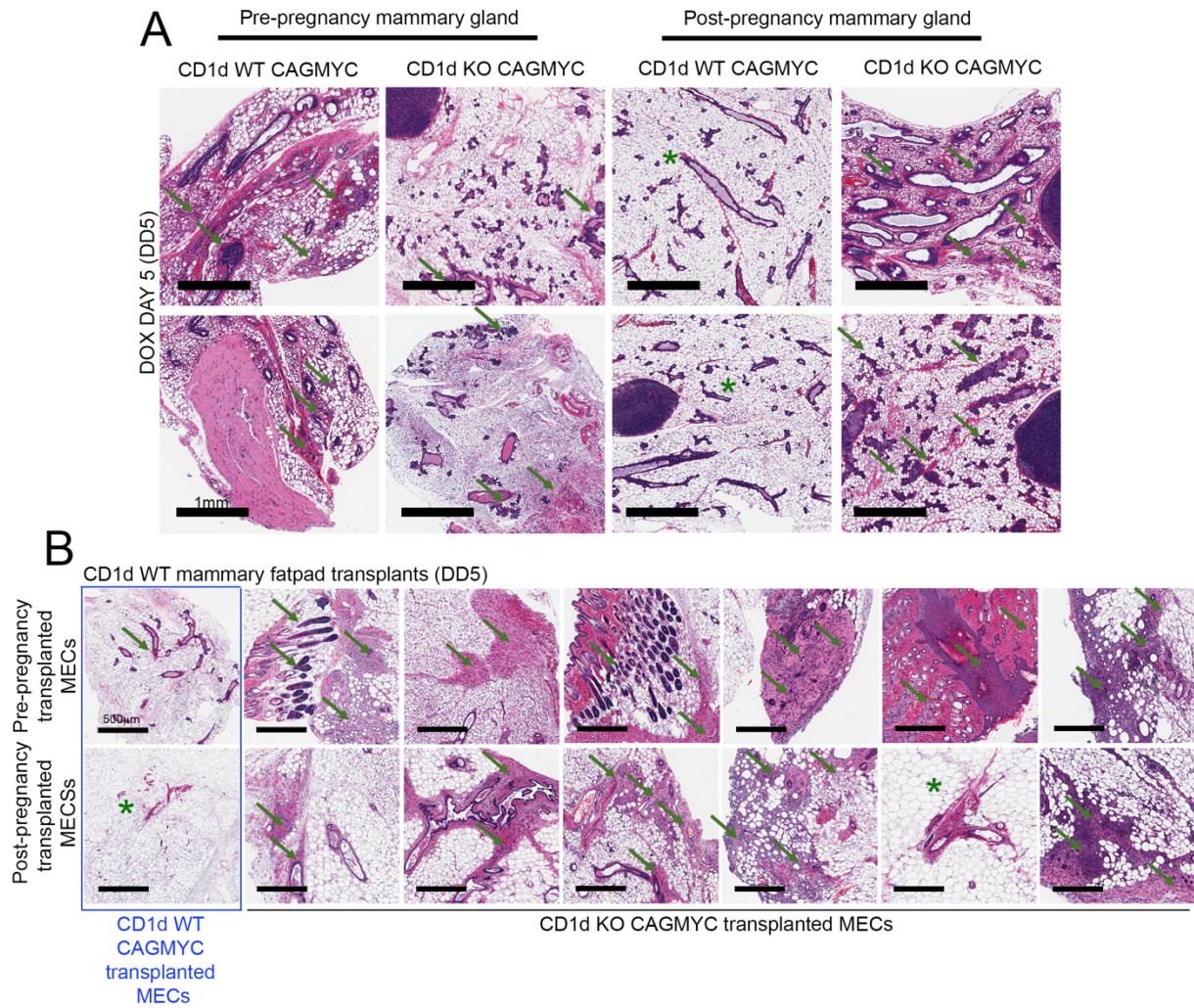


Figure 4

604

605



606

Figure 5

607

608 Main Figure Legends

609 **Figure 1. Single cell analysis identifies transcriptional programs and immune cellular**
610 **heterogeneity in mammary tissue from parous female mice. (A)** UMAP showing epithelial-
611 focused re-clustering (Epcam+, Krt8+, Krt18+, and Krt5+ cells) of pre- and post-pregnancy MECs.
612 **(B)** mRNA levels of senescence-associated, immune communication genes *Cxcl1*, *Ccl2*, *Ilf6*,
613 *Cxcl5*, *Mhc-ii* and *Cd1d* in pre- and post-pregnancy MECs. **(C)** UMAP showing T-cell focused re-
614 clustering (CD3e+ cells) of pre- and post-pregnancy mammary resident immune cells. **(D)** Feature
615 plots showing the expression of T cell markers Cd4, Cd8, Klrk1 and Gzma. **(E)** Dendrogram
616 clustering and dot plot showing molecular signature and lineage identity of pre- and post-
617 pregnancy mammary resident CD3+ immune cells.

618 **Figure 2. Pregnancy induces expansion of specific populations of NKT cells. (A)** Flow
619 cytometry analysis of resident CD45+ cells harvested from pre- and post-pregnancy mammary
620 tissue, and their distribution of NKT cells (NK1.1+CD3+). n=5 nulliparous and 5 parous female
621 mice. *p=0.0004. **(B)** Flow cytometry analysis of the classical NKT cell markers T-bet, CD335,
622 and IFN γ in NKT cells harvested from pre- and post-pregnancy mammary tissue. For Tbet
623 analysis n=4 nulliparous and 4 parous female mice. *p=0.016. For CD335 analysis n=7
624 nulliparous and 7 parous female mice. *p=0.03. **(C)** Flow cytometry analysis of β and $\gamma\delta$ T-cell
625 receptors (TCRs) of pre- and post-pregnancy mammary NKT cells. n=5 nulliparous and 5 parous
626 female mice. *p=0.005. **(D)** Gene set enrichment analysis of differentially expressed genes in
627 FACS-isolated NKT cells from pre- and post-pregnancy mammary tissue. **(E)** Venn-diagram
628 demonstrating the number of shared and exclusive ATAC-seq peaks of FACS-isolated NKT cells
629 from nulliparous female mice (blue circle) and parous female mice (orange circle). **(F)** Genome
630 browser tracks showing distribution of MACS-called ATAC-seq peaks at the *Pdk4*, *Maged1* and
631 *Lypla1* genomic loci from pre- and post-pregnancy NKT cells. For all analyses, error bars indicate
632 standard error of mean across samples of the same experimental group. Statistically significant
633 differences were considered with Student's t-test *p*-value lower than 0.05 (*p*<0.05).

634 **Figure 3. NKT expansion depends on CD1d expression on post-pregnancy MECs. (A)** Flow
635 cytometry analysis of myoepithelial and luminal MECs harvested from pre-pregnancy (and post-
636 pregnancy mammary tissue, and their distribution based on CD1d cell-surface expression. **(B)**
637 Flow cytometry quantification of CD1d+ MECs harvested from pre-pregnancy (black bars, n=8)
638 and post-pregnancy (pink bars, n=10) mammary tissue. *p=0.0036 for luminal MECs and
639 **p=0.0006 for myoepithelial MECs. **(C)** Genome browser tracks showing MACS-called, H3K27ac
640 ChIP-seq peaks at the *Cd1d* genomic locus in FACS-isolated, pre- and post-pregnancy luminal
641 MECs. **(D)** H&E stained histological images and duct quantification from mammary glands
642 harvested from nulliparous (top left, n=6) and parous (bottom left, n=7) CD1d WT female mice,
643 and nulliparous (top right, n=6) and parous (bottom right, n=7) CD1d KO female mice. p=0.86 for
644 pre-pregnancy glands and p=0.78 for post-pregnancy glands. Scale: 7mm. Zoom in panels, scale
645 500 μ m. **(E)** Flow cytometry analysis of mammary resident CD45+ cells harvested from pre- and
646 post-pregnancy CD1d KO female mice, and their distribution of NKT cells (NK1.1+CD3+). n=4
647 nulliparous and n=4 parous female mice. *p=0.3. **(F)** Flow cytometry analysis of α and $\gamma\delta$ T-cell
648 receptors (TCRs) of CD1d KO NKT cells from nulliparous (left, n=3) and parous (right, n=3) female
649 mice. *p=0.5. For all analyses, error bars indicate standard error of mean across samples of the
650 same experimental group. Statistically significant differences were considered with Student's t-
651 test *p*-value lower than 0.05 (*p*<0.05).

652 **Figure 4. Lack of mammary oncogenesis is marked by NKT expansion and CD1d+ MECs**
653 **in CAGMYC and Brca1 KO parous female mice. (A)** Flow cytometry analysis of mammary
654 resident NKT cells (CD45+NK1.1+CD3+) from DOX-treated nulliparous (left panel, n=5) and
655 parous (right panel, n=5) CAGMYC female mice. *p=0.002. **(B)** Flow cytometry quantification of

656 CD1d+ luminal and myoepithelial MECs from DOX-treated nulliparous (left panel, n=16) and
657 parous (right panel, n=11) CAGMYC female mice. *p=0.02. (C) Mammary tumor-free survival plot
658 of nulliparous (black line, n=5) and parous (pink line, n=5) Brca1 KO female mice. (D) H&E stained
659 histological images from mammary tissue and mammary tumor harvested from nulliparous (top
660 panels) and parous (bottom panels) Brca1 KO female mice. (E) Flow cytometry quantification of
661 CD1d+ CD24^{high} luminal MECs from Brca1 KO pre-pregnancy mammary tumors (black bar, n=3),
662 Brca1 KO post-pregnancy healthy mammary tissue (pink bar, n=4), and Brca1 KO post-
663 pregnancy mammary tumor (blue bar, n=1). *p=0.02. (F) Flow cytometry analysis of mammary
664 resident NKT cells in normal mammary tissue from nulliparous, tumor-bearing, Brca1 KO female
665 mice (left panel, n=4) and normal mammary tissue from healthy parous Brca1 KO female mice
666 (right panel, n=4). *p=0.003. (G) Quantification of $\gamma\delta$ NKT cells in normal mammary tissue from
667 nulliparous, tumor-bearing, Brca1 KO female mice (black bar panel, n=4), in mammary tumor
668 tissue from nulliparous Brca1 KO female mice (blue bar, n=3), and in normal mammary tissue
669 from healthy parous Brca1 KO female mice (black bar panel, n=2). *p=0.023 and **p=0.008. For
670 all analyses, error bars indicate standard error of mean across samples of the same experimental
671 group. Statistically significant differences were considered with Student's t-test p-value lower than
672 0.05 (p<0.05).

673 **Figure 5. Functionally active NKT cells are required to block malignant progression of**
674 **post-pregnancy MECs.** (A) H&E stained histological images of mammary tissue harvested from
675 DOX-treated (DD5), nulliparous CD1d WT CAGMYC (far left panels), nulliparous CD1d KO
676 CAGMYC (left panels), parous CD1d WT CAGMYC (right panels), and parous CD1d KO
677 CAGMYC (far right panels) female mice. Green arrows indicate signs of malignant
678 lesions/mammary hyperplasia. Green asterisks indicate normal-like ductal structures. (B) H&E
679 stained histological images of DOX-treated, CD1d WT mammary tissue transplanted with pre-
680 pregnancy CD1d WT CAGMYC MECs (blue font, top far left panel), pre-pregnancy CD1d KO
681 CAGMYC MECs (black font, top panel), post-pregnancy CD1d WT CAGMYC MECs (blue font,
682 bottom far left panel), or post-pregnancy CD1d KO CAGMYC MECs (black font, bottom panel).
683 Green arrows indicate signs of malignant lesions/mammary hyperplasia. Green asterisks indicate
684 normal-like ductal structures.

685

686

687

688

689 **References**

- 690 Almishri, W., Santodomingo-Garzon, T., Le, T., Stack, D., Mody, C.H., and Swain, M.G. (2016).
691 TNF α Augments Cytokine-Induced NK Cell IFN γ Production through TNFR2. *Journal of Innate*
692 *Immunity*.
693
- 694 Bach, K., Pensa, S., Grzelak, M., Hadfield, J., Adams, D.J., Marioni, J.C., and Khaled, W.T.
695 (2017). Differentiation dynamics of mammary epithelial cells revealed by single-cell RNA
696 sequencing. *Nature Communications*.
697
- 698 Bach, K., Pensa, S., Zarocsinceva, M., Kania, K., Stockis, J., Pinaud, S., Lazarus, K.A., Shehata,
699 M., Simões, B.M., Greenhalgh, A.R., et al. (2021). Time-resolved single-cell analysis of Brca1
700 associated mammary tumorigenesis reveals aberrant differentiation of luminal progenitors.
701 *Nature Communications*.
702
- 703 Balato, A., Unutmaz, D., and Gaspari, A.A. (2009). Natural killer T cells: An unconventional t-cell
704 subset with diverse effector and regulatory functions. *Journal of Investigative Dermatology*.
705
- 706 Beyaz, S., Kim, J.H., Pinello, L., Xifaras, M.E., Hu, Y., Huang, J., Kerényi, M.A., Das, P.P., Barnitz,
707 R.A., Herault, A., et al. (2017). The histone demethylase UTX regulates the lineage-specific
708 epigenetic program of invariant natural killer T cells. *Nature Immunology*.
709
- 710 Blakely, C.M., Stoddard, A.J., Belka, G.K., Dugan, K.D., Notarfrancesco, K.L., Moody, S.E.,
711 D’Cruz, C.M., and Chodosh, L.A. (2006). Hormone-induced protection against mammary
712 tumorigenesis is conserved in multiple rat strains and identifies a core gene expression signature
713 induced by pregnancy. *Cancer Research*.
714
- 715 Bochtler, P., Kröger, A., Schirmbeck, R., and Reimann, J. (2008). Type I IFN-Induced, NKT Cell-
716 Mediated Negative Control of CD8 T Cell Priming by Dendritic Cells. *The Journal of Immunology*.
717
- 718 Braig, M., and Schmitt, C.A. (2006). Oncogene-induced senescence: Putting the brakes on tumor
719 development. *Cancer Research*.
720
- 721 Britt, K., Ashworth, A., and Smalley, M. (2007). Pregnancy and the risk of breast cancer.
722 *Endocrine-Related Cancer*.
723
- 724 Brodie, S.G., Xu, X., Qiao, W., Li, W.M., Cao, L., and Deng, C.X. (2001). Multiple genetic changes
725 are associated with mammary tumorigenesis in Brca1 conditional knockout mice. *Oncogene*.
726
- 727 Castillo-Martin, M., Domingo-Domenech, J., Karni-Schmidt, O., Matos, T., and Cordon-Cardo, C.
728 (2010). Molecular pathways of urothelial development and bladder tumorigenesis. *Urologic*
729 *Oncology: Seminars and Original Investigations*.
730
- 731 Chan, S.H., Tsai, K.W., Chiu, S.Y., Kuo, W.H., Chen, H.Y., Jiang, S.S., Chang, K.J., Hung, W.C.,
732 and Wang, L.H. (2019). Identification of the novel role of CD24 as an oncogenesis regulator and
733 therapeutic target for triple-negative breast cancer. *Molecular Cancer Therapeutics*.
734
- 735 Chen, Y., and Olopade, O.I. (2008). MYC in breast tumor progression. *Expert Review of*
736 *Anticancer Therapy*.
737

- 738 Chung, C.Y., Ma, Z., Dravis, C., Preissl, S., Poirion, O., Luna, G., Hou, X., Giraddi, R.R., Ren, B.,
739 and Wahl, G.M. (2019). Single-Cell Chromatin Analysis of Mammary Gland Development Reveals
740 Cell-State Transcriptional Regulators and Lineage Relationships. *Cell Reports*.
741
- 742 Ciccone, M.F., Trousdell, M.C., and dos Santos, C.O. (2020). Characterization of Organoid
743 Cultures to Study the Effects of Pregnancy Hormones on the Epigenome and Transcriptional
744 Output of Mammary Epithelial Cells. *Journal of Mammary Gland Biology and Neoplasia*.
745
- 746 Connaughton, S., Chowdhury, F., Attia, R.R., Song, S., Zhang, Y., Elam, M.B., Cook, G.A., and
747 Park, E.A. (2010). Regulation of pyruvate dehydrogenase kinase isoform 4 (PDK4) gene
748 expression by glucocorticoids and insulin. *Molecular and Cellular Endocrinology*.
749
- 750 Coussens, L.M., and Pollard, J.W. (2011). Leukocytes in mammary development and cancer.
751 *Cold Spring Harbor Perspectives in Biology*.
752
- 753 Dawson, C.A., Pal, B., Vaillant, F., Gandolfo, L.C., Liu, Z., Bleriot, C., Ginhoux, F., Smyth, G.K.,
754 Lindeman, G.J., Mueller, S.N., et al. (2020). Tissue-resident ductal macrophages survey the
755 mammary epithelium and facilitate tissue remodelling. *Nature Cell Biology*.
756
- 757 Doisne, J.M., Bartholin, L., Yan, K.P., Garcia, C.N., Duarte, N., Le Luduec, J.B., Vincent, D.,
758 Cyprian, F., Horvat, B., Martel, S., et al. (2009). iNKT cell development is orchestrated by different
759 branches of TGF- β signaling. *Journal of Experimental Medicine*.
760
- 761 Faunce, D.E., Palmer, J.L., Paskowicz, K.K., Witte, P.L., and Kovacs, E.J. (2005). CD1d-
762 Restricted NKT Cells Contribute to the Age-Associated Decline of T Cell Immunity. *The Journal*
763 *of Immunology*.
764
- 765 Feigman, M.J., Moss, M.A., Chen, C., Cyrill, S.L., Ciccone, M.F., Trousdell, M.C., Yang, S.T.,
766 Frey, W.D., Wilkinson, J.E., and dos Santos, C.O. (2020). Pregnancy reprograms the epigenome
767 of mammary epithelial cells and blocks the development of premalignant lesions. *Nature*
768 *Communications*.
769
- 770 Fornetti, J., Martinson, H., Borges, V., and Schedin, P. (2012). Emerging targets for the prevention
771 of pregnancy-associated breast cancer. *Cell Cycle*.
772
- 773 Freire-de-Lima, C.G., Yi, Q.X., Gardai, S.J., Bratton, D.L., Schiemann, W.P., and Henson, P.M.
774 (2006). Apoptotic cells, through transforming growth factor- β , coordinately induce anti-
775 inflammatory and suppress pro-inflammatory eicosanoid and NO synthesis in murine
776 macrophages. *Journal of Biological Chemistry*.
777
- 778 Gapin, L., Godfrey, D.I., and Rossjohn, J. (2013). Natural Killer T cell obsession with self-antigens.
779 *Current Opinion in Immunology*.
780
- 781 Germanov, E., Veinotte, L., Cullen, R., Chamberlain, E., Butcher, E.C., and Johnston, B. (2008).
782 Critical Role for the Chemokine Receptor CXCR6 in Homeostasis and Activation of CD1d-
783 Restricted NKT Cells. *The Journal of Immunology*.
784
- 785 Godfrey, D.I., MacDonald, H.R., Kronenberg, M., Smyth, M.J., and Van Kaer, L. (2004). NKT
786 cells: What's in a name? *Nature Reviews Immunology*.
787

788 Grushko, T.A., Dignam, J.J., Das, S., Blackwood, A.M., Perou, C.M., Ridderstråle, K.K.,
789 Anderson, K.N., Wei, M.J., Adams, A.J., Hagos, F.G., et al. (2004). MYC Is Amplified in BRCA1-
790 Associated Breast Cancers. *Clinical Cancer Research*.
791
792 Guo, Q., Betts, C., Pennock, N., Mitchell, E., and Schedin, P. (2017). Mammary Gland Involution
793 Provides a Unique Model to Study the TGF- β Cancer Paradox. *Journal of Clinical Medicine*.
794
795 Henry, S., Trousdell, M.C., Cyrill, S.L., Zhao, Y., Feigman, Mary.J., Bouhuis, J.M., Aylard, D.A.,
796 Siepel, A., and dos Santos, C.O. (2021). Characterization of Gene Expression Signatures for the
797 Identification of Cellular Heterogeneity in the Developing Mammary Gland. *Journal of Mammary*
798 *Gland Biology and Neoplasia*.
799
800 Hitchcock, J.R., Hughes, K., Harris, O.B., and Watson, C.J. (2020). Dynamic architectural
801 interplay between leucocytes and mammary epithelial cells. *FEBS Journal 287*.
802
803 Huber, S. (2015). ER α ² and ER α ± Differentially Regulate NKT and V α ³4+ T-cell
804 Activation and T-regulatory Cell Response in Coxsackievirus B3 Infected Mice. *Journal of Clinical*
805 *& Cellular Immunology*.
806
807 Huh, S.J., Clement, K., Jee, D., Merlini, A., Choudhury, S., Maruyama, R., Yoo, R., Chytil, A.,
808 Boyle, P., Ran, F.A., et al. (2015). Age- and pregnancy-associated dna methylation changes in
809 mammary epithelial cells. *Stem Cell Reports*.
810
811 Ibrahim, A.M., Moss, M.A., Gray, Z., Rojo, M.D., Burke, C.M., Schwertfeger, K.L., dos Santos,
812 C.O., and Machado, H.L. (2020). Diverse Macrophage Populations Contribute to the Inflammatory
813 Microenvironment in Premalignant Lesions During Localized Invasion. *Frontiers in Oncology*
814
815 Jehmlich, U., Alahmad, A., Biedenweg, D., and Hundt, M. (2013). The role of palmitoyl-protein
816 thioesterases in T cell activation (P1398). *The Journal of Immunology 190*, 204.2 LP-204.2.
817
818 Kale, A., Sharma, A., Stolzing, A., Stolzing, A., Desprez, P.Y., Desprez, P.Y., Campisi, J., and
819 Campisi, J. (2020). Role of immune cells in the removal of deleterious senescent cells. *Immunity*
820 *and Ageing*.
821
822 Kordon, E.C., and Coso, O.A. (2017). Postlactational Involution: Molecular Mechanisms and
823 Relevance for Breast Cancer Development. In *Current Topics in Lactation*.
824
825 Lee, Y.J., Starrett, G.J., Lee, S.T., Yang, R., Henzler, C.M., Jameson, S.C., and Hogquist, K.A.
826 (2016). Lineage-Specific Effector Signatures of Invariant NKT Cells Are Shared amongst $\gamma\delta$ T,
827 Innate Lymphoid, and Th Cells. *The Journal of Immunology*.
828
829 Li, C.M.C., Shapiro, H., Tsiobikas, C., Selfors, L.M., Chen, H., Rosenbluth, J., Moore, K., Gupta,
830 K.P., Gray, G.K., Oren, Y., et al. (2020a). Aging-Associated Alterations in Mammary Epithelia and
831 Stroma Revealed by Single-Cell RNA Sequencing. *Cell Reports*.
832
833 Li, S., Gestl, S.A., and Gunther, E.J. (2020b). A multistage murine breast cancer model reveals
834 long-lived premalignant clones refractory to parity-induced protection. *Cancer Prevention*
835 *Research*.
836

- 837 Lyons, T.R., O'Brien, J., Borges, V.F., Conklin, M.W., Keely, P.J., Eliceiri, K.W., Marusyk, A., Tan,
838 A.C., and Schedin, P. (2011). Postpartum mammary gland involution drives progression of ductal
839 carcinoma in situ through collagen and COX-2. *Nature Medicine*.
840
- 841 Macho-Fernandez, E., and Brigl, M. (2015). The extended family of CD1d-restricted NKT cells:
842 Sifting through a mixed bag of TCRs, antigens, and functions. *Frontiers in Immunology*.
843
- 844 Majumdar, D., Tiernan, J.P., Lobo, A.J., Evans, C.A., and Corfe, B.M. (2012). Keratins in
845 colorectal epithelial function and disease. *International Journal of Experimental Pathology*.
846
- 847 Mantell, B.S., Stefanovic-Racic, M., Yang, X., Dedousis, N., Sipula, I.J., and O'Doherty, R.M.
848 (2011). mice lacking NKT cells but with a complete complement of CD8+ T-Cells are not protected
849 against the metabolic abnormalities of diet-induced obesity. *PLoS ONE*.
850
- 851 Martinson, H.A., Jindal, S., Durand-Rougely, C., Borges, V.F., and Schedin, P. (2015). Wound
852 healing-like immune program facilitates postpartum mammary gland involution and tumor
853 progression. *International Journal of Cancer*.
854
- 855 Medina, D., and Kittrell, F.S. (2003). p53 function is required for hormone-mediated protection of
856 mouse mammary tumorigenesis. *Cancer Research*.
857
- 858 Medina, D., Come, S., Santen, R., Ellis, M., Green, J., Nicholson, R., Brown, M., and Lee, A.
859 (2004). Breast Cancer: The Protective Effect of Pregnancy. In *Clinical Cancer Research*, p.
860 Mincheva-Nilsson, L. (2003). Pregnancy and gamma/delta T cells: Taking on the hard questions.
861 *Reproductive Biology and Endocrinology*.
862
- 863 Mombaerts, P., Iacomini, J., Johnson, R.S., Herrup, K., Tonegawa, S., and Papaioannou, V.E.
864 (1992). RAG-1-deficient mice have no mature B and T lymphocytes. *Cell*.
865
- 866 Mycko, M.P., Ferrero, I., Wilson, A., Jiang, W., Bianchi, T., Trumpp, A., and MacDonald, H.R.
867 (2009). Selective Requirement for c-Myc at an Early Stage of V α 14i NKT Cell Development. *The*
868 *Journal of Immunology*.
869
- 870 Na, Y.R., Jung, D., Song, J., Park, J.W., Hong, J.J., and Seok, S.H. (2020). Pyruvate
871 dehydrogenase kinase is a negative regulator of interleukin-10 production in macrophages.
872 *Journal of Molecular Cell Biology*.
873
- 874 Nichols, H.B., Schoemaker, M.J., Cai, J., Xu, J., Wright, L.B., Brook, M.N., Jones, M.E., Adami,
875 H.O., Baglietto, L., Bertrand, K.A., et al. (2019). Breast cancer risk after recent childbirth: A pooled
876 analysis of 15 prospective studies. *Annals of Internal Medicine*.
877
- 878 O'Brien, J., Lyons, T., Monks, J., Lucia, M.S., Wilson, R.S., Hines, L., Man, Y.G., Borges, V., and
879 Schedin, P. (2010). Alternatively activated macrophages and collagen remodeling characterize
880 the postpartum involuting mammary gland across species. *American Journal of Pathology*.
881
- 882 Oh, S.J., Ahn, S., Jin, Y.-H., Ishifune, C., Kim, J.H., Yasutomo, K., and Chung, D.H. (2015). Notch
883 1 and Notch 2 synergistically regulate the differentiation and function of invariant NKT cells.
884 *Journal of Leukocyte Biology*.
885

- 886 Pal, B., Chen, Y., Vaillant, F., Jamieson, P., Gordon, L., Rios, A.C., Wilcox, S., Fu, N., Liu, K.H.,
887 Jackling, F.C., et al. (2017). Construction of developmental lineage relationships in the mouse
888 mammary gland by single-cell RNA profiling. *Nature Communications*.
889
- 890 Pal, B., Chen, Y., Milevskiy, M.J.G., Vaillant, F., Prokopuk, L., Dawson, C.A., Capaldo, B.D.,
891 Song, X., Jackling, F., Timpson, P., et al. (2021). Single cell transcriptome atlas of mouse
892 mammary epithelial cells across development. *Breast Cancer Research*.
893
- 894 Plaks, V., Boldajipour, B., Linnemann, J.R., Nguyen, N.H., Kersten, K., Wolf, Y., Casbon, A.J.,
895 Kong, N., van den Bijgaart, R.J.E., Sheppard, D., et al. (2015). Adaptive Immune Regulation of
896 Mammary Postnatal Organogenesis. *Developmental Cell*.
897
- 898 Rahat, M.A., Coffelt, S.B., Granot, Z., Muthana, M., and Amedei, A. (2016). Macrophages and
899 Neutrophils: Regulation of the Inflammatory Microenvironment in Autoimmunity and Cancer.
900 *Mediators of Inflammation*.
901
- 902 Ricciardelli, C., Lokman, N.A., Pyragius, C.E., Ween, M.P., Macpherson, A.M., Ruszkiewicz, A.,
903 Hoffmann, P., and Oehler, M.K. (2017). Keratin 5 overexpression is associated with serous
904 ovarian cancer recurrence and chemotherapy resistance. *Oncotarget*.
905
- 906 Rizvi, Z.A., Puri, N., and Saxena, R.K. (2015). Lipid antigen presentation through CD1d pathway
907 in mouse lung epithelial cells, macrophages and dendritic cells and its suppression by poly-
908 dispersed single-walled carbon nanotubes. *Toxicology in Vitro* 29.
909
- 910 Saeki, K., Chang, G., Kanaya, N., Wu, X., Wang, J., Bernal, L., Ha, D., Neuhausen, S.L., and
911 Chen, S. (2021). Mammary cell gene expression atlas links epithelial cell remodeling events to
912 breast carcinogenesis. *Communications Biology*.
913
- 914 dos Santos, C.O., Rebbeck, C., Rozhkova, E., Valentine, A., Samuels, A., Kadiri, L.R., Osten, P.,
915 Harris, E.Y., Uren, P.J., Smith, A.D., et al. (2013). Molecular hierarchy of mammary differentiation
916 yields refined markers of mammary stem cells. *Proceedings of the National Academy of Sciences*
917 *of the United States of America*.
918
- 919 dos Santos, C.O., Dolzhenko, E., Hodges, E., Smith, A.D., and Hannon, G.J. (2015). An
920 Epigenetic Memory of Pregnancy in the Mouse Mammary Gland. *Cell Reports*.
921
- 922 Savage, A.K., Constantinides, M.G., Han, J., Picard, D., Martin, E., Li, B., Lantz, O., and
923 Bendelac, A. (2008). The Transcription Factor PLZF Directs the Effector Program of the NKT Cell
924 Lineage. *Immunity*.
925
- 926 Schwertfeger, K.L., Richert, M.M., and Anderson, S.M. (2001). Mammary gland involution is
927 delayed by activated Akt in transgenic mice. *Molecular Endocrinology*.
928
- 929 Seiler, M.P., Mathew, R., Liszewski, M.K., Spooner, C., Barr, K., Meng, F., Singh, H., and
930 Bendelac, A. (2012). Elevated and sustained expression of the transcription factors Egr1 and
931 Egr2 controls NKT lineage differentiation in response to TCR signaling. *Nature Immunology*.
932
- 933 Sivaraman, L., Conneely, O.M., Medina, D., and O'Malley, B.W. (2001). p53 is a potential
934 mediator of pregnancy and hormone-induced resistance to mammary carcinogenesis.
935 *Proceedings of the National Academy of Sciences of the United States of America*.
936

- 937 Stewart, T.A., Hughes, K., Hume, D.A., and Davis, F.M. (2019). Developmental Stage-Specific
938 Distribution of Macrophages in Mouse Mammary Gland. *Frontiers in Cell and Developmental*
939 *Biology*.
940
- 941 Sulahian, R., Chen, J., Arany, Z., Jadhav, U., Peng, S., Rustgi, A.K., Bass, A.J., Srivastava, A.,
942 Hornick, J.L., and Shivdasani, R.A. (2015). SOX15 Governs Transcription in Human Stratified
943 Epithelia and a Subset of Esophageal Adenocarcinomas. *CMGH*.
944
- 945 Terry, M.B., Liao, Y., Kast, K., Antoniou, A.C., McDonald, J.A., Mooij, T.M., Engel, C., Nogues,
946 C., Buecher, B., Mari, V., et al. (2018). The Influence of Number and Timing of Pregnancies on
947 Breast Cancer Risk for Women With BRCA1 or BRCA2 Mutations. *JNCI Cancer Spectrum*.
948
- 949 Thibeault, S.L., Rees, L., Pazmany, L., and Birchall, M.A. (2009). At the crossroads: Mucosal
950 immunology of the larynx. *Mucosal Immunology*.
951
- 952 Townsend, M.J., Weinmann, A.S., Matsuda, J.L., Salomon, R., Farnham, P.J., Biron, C.A., Gapin,
953 L., and Glimcher, L.H. (2004). T-bet regulates the terminal maturation and homeostasis of NK
954 and V α 14i NKT cells. *Immunity*.
955
- 956 Wang, Y., Chaffee, T.S., Larue, R.S., Huggins, D.N., Witschen, P.M., Ibrahim, A.M., Nelson, A.C.,
957 Machado, H.L., and Schwertfeger, K.L. (2020). Tissue-resident macrophages promote
958 extracellular matrix homeostasis in the mammary gland stroma of nulliparous mice. *ELife*.
959
- 960 Wu, Y., Kyle-Cezar, F., Woolf, R.T., Naceur-Lombardelli, C., Owen, J., Biswas, D., Lorenc, A.,
961 Vantourout, P., Gazinska, P., Grigoriadis, A., et al. (2019). An innate-like V δ 1+ $\gamma\delta$ T cell
962 compartment in the human breast is associated with remission in triple-negative breast cancer.
963 *Science Translational Medicine*.
964
- 965 Yu, J., Mitsui, T., Wei, M., Mao, H., Butchar, J.P., Shah, M.V., Zhang, J., Mishra, A., Alvarez-
966 Breckenridge, C., Liu, X., et al. (2011). NKp46 identifies an NKT cell subset susceptible to
967 leukemic transformation in mouse and human. *Journal of Clinical Investigation*.
968
- 969 Zhang, Y., Springfield, R., Chen, S., Li, X., Feng, X., Moshirian, R., Yang, R., and Yuan, W.
970 (2019). α -GalCer and iNKT cell-based cancer immunotherapy: Realizing the therapeutic
971 potentials. *Frontiers in Immunology*.
972